Field tests of 3-component geophones, Part II

Don C. Lawton and Malcolm B. Bertram

SUMMARY

Tests of Geosource, Litton, Oyo and Omniphones^{TM} 3-component geophones showed similar performance characteristics for all geophones for test signals generated by a vector source at a horizontal distance of 10 m from the geophones. All geophones showed good separation between components, although the horizontal components of the Omniphones were found to be noisier than those of the other geophones.

Polarization directions measured by the geophones for a semicircle of shotpoints gave very similar results for all geophones and closely matched the expected azimuths.

INTRODUCTION

In 1990, a field experimental program was undertaken to examine the relative performance of several different types of 3-component geophones. The results of the first experiment, involving Litton, Geosource and Oyo geophones, were reported by Lawton and Bertram (1990) and showed that these geophones all recorded very similar waveforms for an input signal created by a small explosive charge. These geophones have elements which are arranged in a cartesian configuration, and no cross-coupling between the elements was recorded during the tests.

A second experiment was undertaken in October, 1990, using the same geophones as were tested in the first experiment, but this time also including two Omniphones. These geophones differ from the other geophones in that the data recorded by the three elements are digitized in the geophone, passed through a polarization filter, and then transmitted sequentially to the seismic recorder through a digital-to-analogue converter. The elements in the Omniphone are arranged in a Gal'perin (trigonal) configuration, with the axes of the elements separated by 120 degrees and tilted at 54.73 degrees from the vertical. However, prior to output, the data in the geophones are rotated into an orthogonal coordinate system.

Some results from the second experiment were presented orally at the 1990 CREWES sponsors meeting in Banff (November 26 to 27, 1990). These results showed consistent behaviour amongst the conventional geophones (Geosource, Litton and Oyo) but some inconsistent amplitude variations between the output traces of the Omniphones. These differences were examined in detail, in conjunction with Terra Linda Canada. Inc., who provided the geophones, but no technical explanation was reached and the test was deemed inconclusive.

In order to resolve the uncertain results from the second experiment, another test was undertaken in February 1991, the results of which are discussed in this report.

DATA ACQUISITION

The experiment was undertaken on February 5, 1991 near the Physical Plant on the University of Calgary campus, using a procedure similar to that described by Lawton and Bertram (1990). The ground encompassing the test area is flat and was well frozen at the time of the experiment. For this experiment, one of each of the Geosource, Litton and Oyo geophones was used, along with two Omniphones. The geophones were clustered (Figure

1) with the long axes of the geophones oriented towards a reference azimuth (defined as 0 degrees). In this report, this axis is designated as H1 and the other, orthogonal axis (oriented to 270 degrees) is designated H2. As an additional test, the direction of one of the Omniphones was reversed; the normal and reversed Omniphones are referred to as Omni-n and Omni-r, respectively. After the photograph shown in Figure 1 was taken, all geophones were packed in snow to minimise wind noise.

The source used for the experiment is shown in Figure 2 and consisted of a sledge hammer and a railway tie which was reinforced with a steel base plate and end caps. The edges of the base plate were cut with a sawtooth pattern to improve coupling of the source to the frozen ground.

Five shotpoints were located at 45 degree increments in a semicircle around the geophone cluster, as shown schematically in Figure 3. A shot circle radius of 10 m was found to be appropriate for maintaining a good signal to noise ratio in the recorded data. At each shotpoint, three different source orientations were used, two horizontal and one vertical (Figure 3). The horizontal modes were radial (R) and tangential (T). In the former mode, the source was struck in a direction toward the shot centre, whereas in the latter mode, the source was struck in clockwise direction and tangential to the shot circle. For the vertical mode (V), the source was struck vertically downwards. All data were recorded at a 2 ms sample interval with Sercel 338HR instruments operating with low-cut and notch filters out. An exact time-break could not be established with the set-up used, and the shot was timed manually to occur in a window between the I/O blaster tone-shift and the internal time-break in the instruments. Hence no velocity information could be obtained from the data.

DATA PROCESSING

The Omniphones had fixed record length of 7 s, yielding 21 s of data for the sequential output trace. In addition, there is a 50 ms gap between the data for each component, as well as a 19 ms delay associated with the polarization filter (D. Miles, pers. comm.) Hence, after demultiplexing, the Omniphone trace was decomposed into three separate traces, representing vertical (V), transverse (H2) and radial (H1) components.

Because the time-break occurred within a 1-second window, a static correction was applied to all records so that the first arrival was fixed at about 100 ms. This correction was constant for all traces within a particular record, but varied between records. Thus, no relative time shifts were applied between traces within a record.

After time-shifting, the data were displayed and it was observed that there were considerable variations in amplitude between records, probably caused by inconsistent source coupling. Also, the Omniphone signal output level is 6 times greater than that of the other types of geophones tested. In order to provide a better visual comparison, the average amplitude of each record was normalised to a fixed value. This scale factor was constant for all traces within a particular record, but varied between records, so that relative amplitudes between traces within a record were preserved. No time-variant scaling was applied to the data.

RESULTS

The time-shifted and normalised data are displayed in Figures 4 to 8 for shotpoints 1 to 5 respectively (azimuths of 0 degrees to 180 degrees at increments of 45 degrees).

Within each record, there are 3 traces from each of 5 geophones, arranged in order (right to left) of Geosource (G), Litton (L), Oyo (O), Omni-n (ON) and Omni-r (OR). For each geophone, again from right to left, the trace order is vertical (V), radial (H1) and transverse (H2). Each shotpoint consists of three separate records, with source orientations of vertical (V), tangential (T) and radial (R), from right to left respectively.

The events recorded are interpreted to be P-wave arrivals, S-wave arrivals or surface waves. Because the ground was frozen, the body waves are probably direct arrivals propagating horizontally through the frozen layer rather than arrivals refracted from a deeper interface. The time delay (about 10 ms) between the vertical and horizontal channels, for a radial source orientation, is consistent with the expected difference between P-wave and surface-wave arrivals for the source- receiver offset of 10 m.

Examination of the data in Figures 4 to 8 show that equivalent traces from all of the geophones exhibit a similar signal character. This visual comparison is assisted by separating the data into common component and common source gathers. Figure 9 is a display of the vertical component gathers for a vertical source orientation. In figure 9, as well as in subsequent common component gathers, the geophone order (right to left) is: Geosource, Litton, Oyo, Omni-n, Omni-r. As expected, the signal character is invariant of the source location and is very similar across all geophones. The residual moveout across each gather is a result of the spatial separation of the geophones in the central cluster (see Figure 1).

Figure 10 contains H1 common component gathers for a radial source orientation at each shotpoint. The amplitude maxima (but opposite polarity) observed at shotpoints 0 degrees and 180 degrees is consistent with the H1 direction (0 degrees). The minimum at 90 degrees results from the orthogonal relationship between the source direction and the H1 direction. Clearly, the Geosource, Litton and Oyo geophones show almost no coupling in this orientation, whereas both Omniphones show some low-level signal. Figure 10 also shows clearly the Omniphone. Data at shotpoints 45 degrees and 135 degrees show intermediate amplitudes and opposite polarities, as expected.

Figure 11 is similar to Figure 10 except that H2 common component gathers are displayed for a tangential source orientation. The matched source and receiver orientations are at shotpoints 0 degrees and 180 degrees and data in these gathers again have the highest amplitudes. It is also noted that the H1 polarity of the Omniphones is opposite to that of the other three types of geophones. The separation between the horizontal components in Figure 11 is not as good as that seen in Figure 10, as indicated by the relatively high amplitude events seen in Figure 11 for shotpoint at 90 degrees.

HODOGRAM ANALYSIS

The particle motion associated with the events recorded are displayed on hodograms. Figures 12 to 16 show particle motion in the horizontal plane (H1 vs. H2) for radial source orientations at each of the 5 shotpoints, from 0 degrees through the 180 degrees respectively. A data window of 100 to 160 ms (30 samples) was selected as this contains the events of interest. In all hodograms in this report, the signs of the H2 component have been normalised to positive displacements in the 270 degree direction (See Figure 3). Figures 12 to 16 show that for the radial source orientation, the particle motion is generally confined to the source-receiver plane and this behaviour is shown very consistently by the Geosource, Litton and Oyo geophones. During this analysis, it was found initially that the Omniphone hodograms showed considerably greater scatter than hodograms from the other types of geophones. Investigation showed that this scatter could be minimised in most

cases by applying a 2ms lag (1 sample) to the H2 trace with respect to the H1 trace. This delay was probably due to the Omniphone and Sercel clocks not being exactly synchronised. Figure 17 shows the rather dramatic effect of lags of up to +/- 4 ms on Omniphone H1 vs H2 hodograms for the radial source mode at 135 degrees. All Omniphone hodograms in this report have had an optimum lag (either 0 or 2 ms) applied. Generally, the long axis of the Omniphone hodograms are rotated slightly clockwise in comparison to those for the other geophones; this may be due to small alignment errors in the field.

Figures 18 to 22 show H1 vs. H2 hodograms for all shotpoints for the tangential source mode. These plots show maximum coupling parallel to the source excitation direction, although some particle motion in the source-receiver plane was also recorded. In this mode, all geophones behaved in a similar manner.

Figure 23 to 25 show V vs. H hodograms for the vertical source mode and particle motion in the source-receiver plane. Hence for the shotpoints at 0 and 180 degrees (Figures 22, 24), V vs. H1 hodograms are plotted, whereas for the shotpoint at 90 degrees (Figure 23), V vs. H2 hodograms are plotted. In all cases, the hodograms clearly show retrograde, elliptical particle motion associated with a Rayleigh wave. The compressed ellipse evident in the Omniphone hodograms is a result of polarization filtering in the geophone.

CONCLUSIONS

From this test program, the following conclusions are drawn:

(a) All geophones tested yielded similar wave forms for all three components.

(b) The cartesian geophones (Gesource, Litton, Oyo) showed excellent separation between components.

(c) The Omniphones showed excellent separation between the vertical and horizontal components. The separation between the horizontal components was acceptable, but was not as good as that achieved by the other geophones. This might be a result of the Gal'perin configuration used in the Omniphones.

(d) The transverse component (H2) of the Omniphones is opposite in polarity to the transverse (H2) component of the Gesource, Litton and Oyo geophones.

(e) There appears to be a lag of up to 2 ms between the H2 and H1 components of the Omniphone after trace reconstruction.

ACKNOWLEDGEMENTS

This research was supported by the CREWES Project using facilities provided by the Department of Geology and Geophysics at the University of Calgary. Assistance with the source and with the field acquisition was provided by Mr. Carl Gunhold, Mr. Eric Gallant and Ms. Susan Miller. Western Geophysical Ltd, Geosource Canada, Oyo-Geospace Canada and Terra Linda Canada, Inc. are thanked for providing geophones for these tests.

REFERENCE

Lawton, D.C. and Bertram, M.B., 1990, Field tests of 3-component geophones; CREWES Research Report, Volume 2, 1-17.

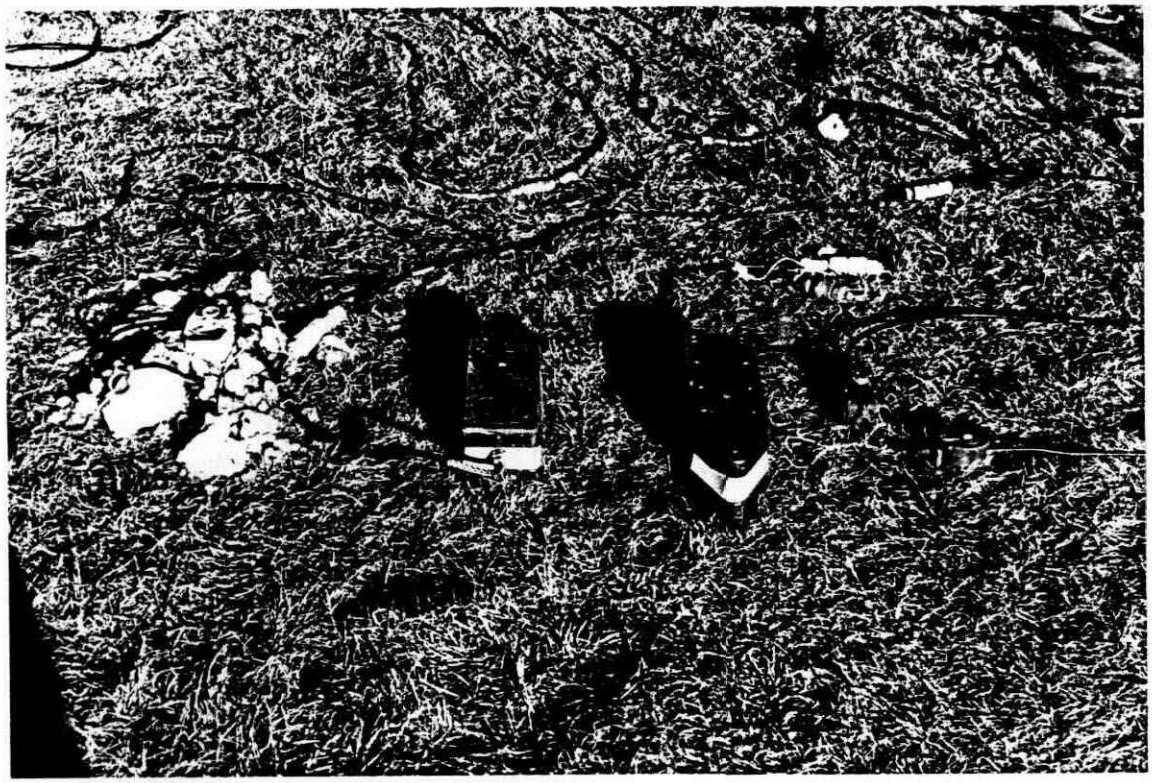

Figure 1. Photograph of geophone cluster used in the experiment. Note that one Omniphone is reversed.

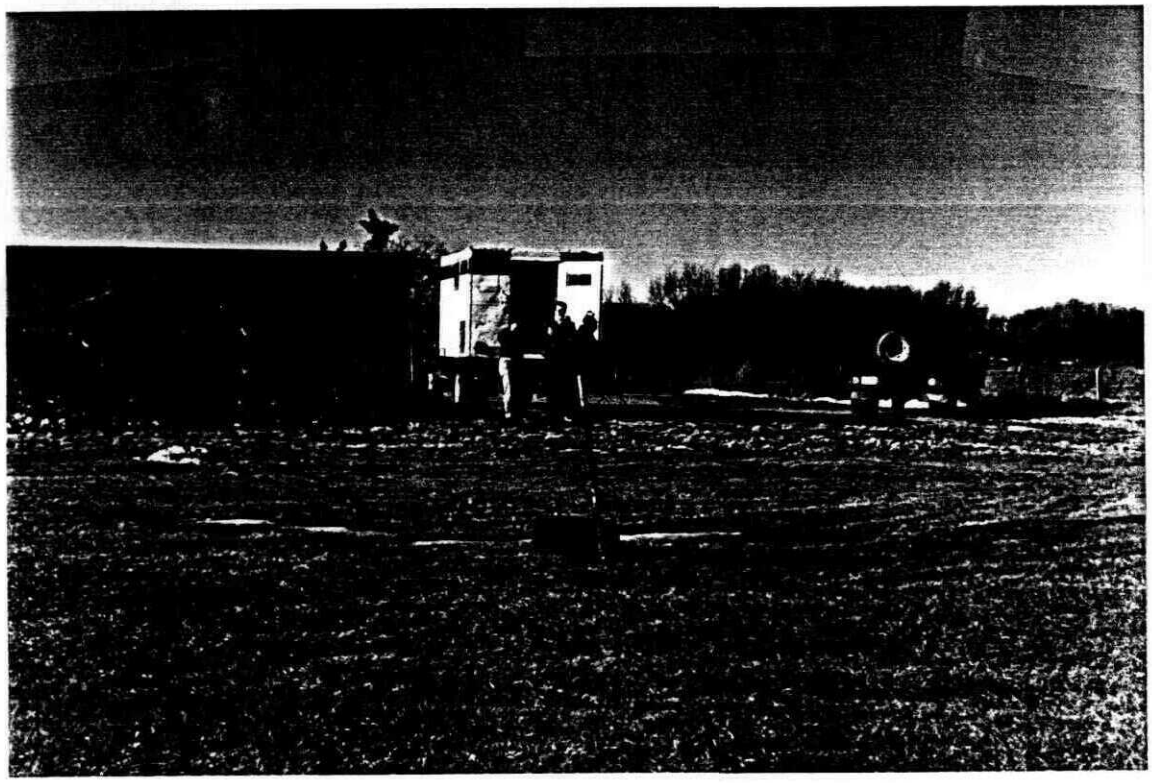

Figure 2. Photograph of the source used in the experiment.

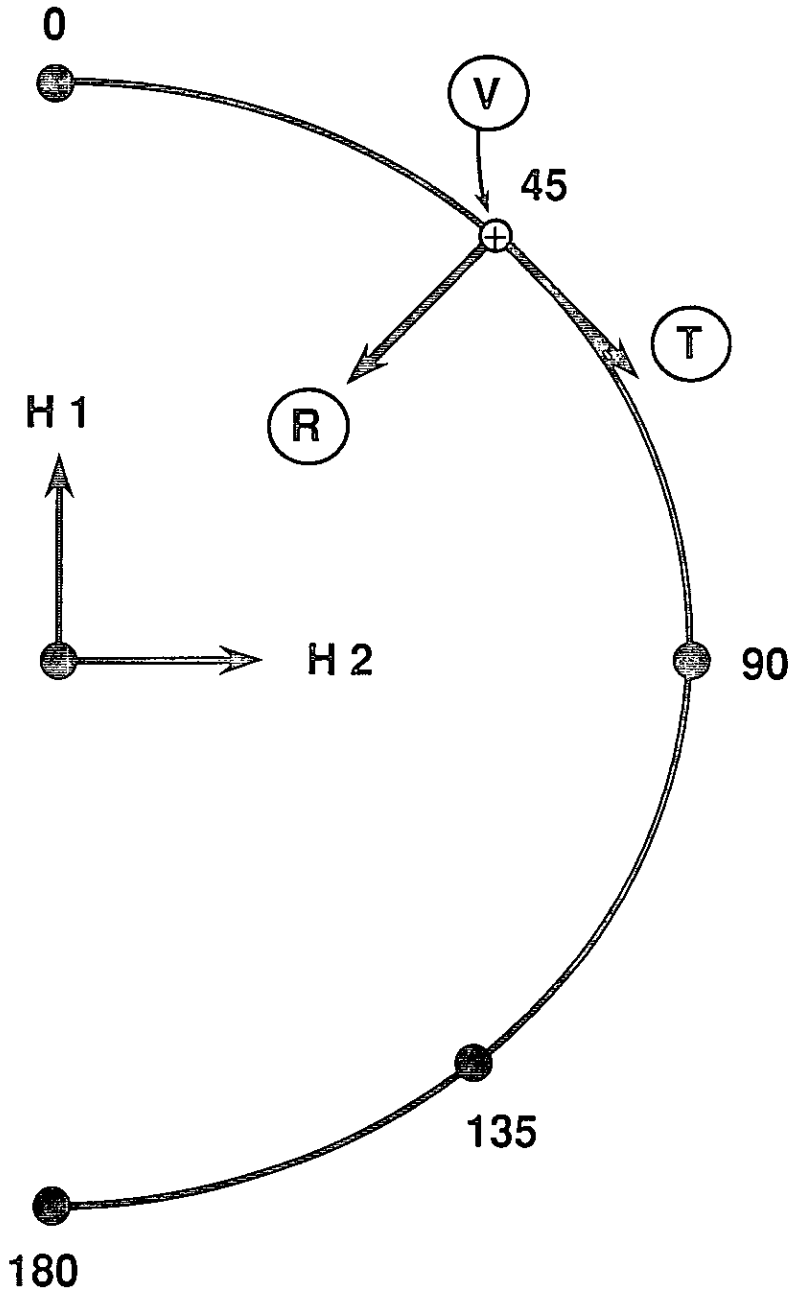

Figure 3. Schematic diagram showing field layout of geophones (centre) and shotpoints. H1 and H2 are defined as the positive directions of the horizontal components of the geophones for hodogram analysis. V, R, and T represent vertical, radial and tangential source modes.

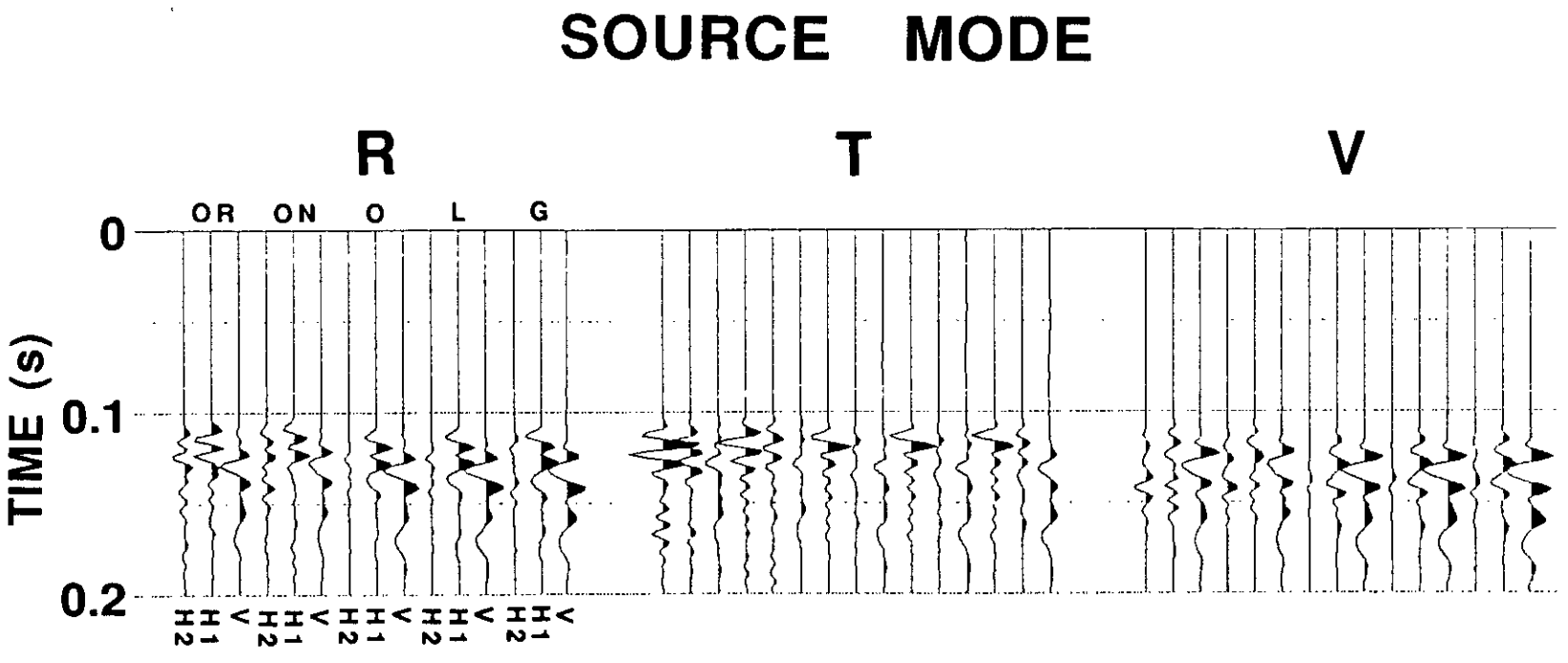

Figure 4. Processed field data from the shotpoint at 0 degrees. Each record contains 3 traces from each of 5 geophones. The geophone order (right to left) is Geosource (G), Litton (L), Oyo (O), Omni-n (ON) and Omni-r (OR). For each geophone, the trace order (right to left) is V, H1, H2.

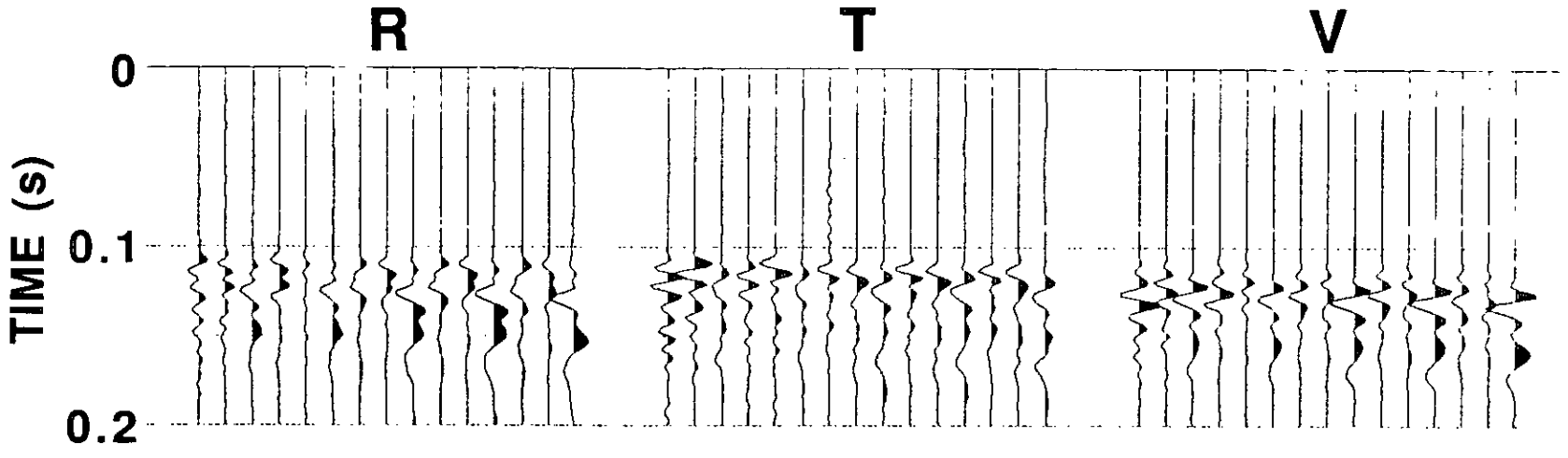

Figure 5. Processed field data from the shotpoint at 45 degrees. Trace order as for Figure 4.

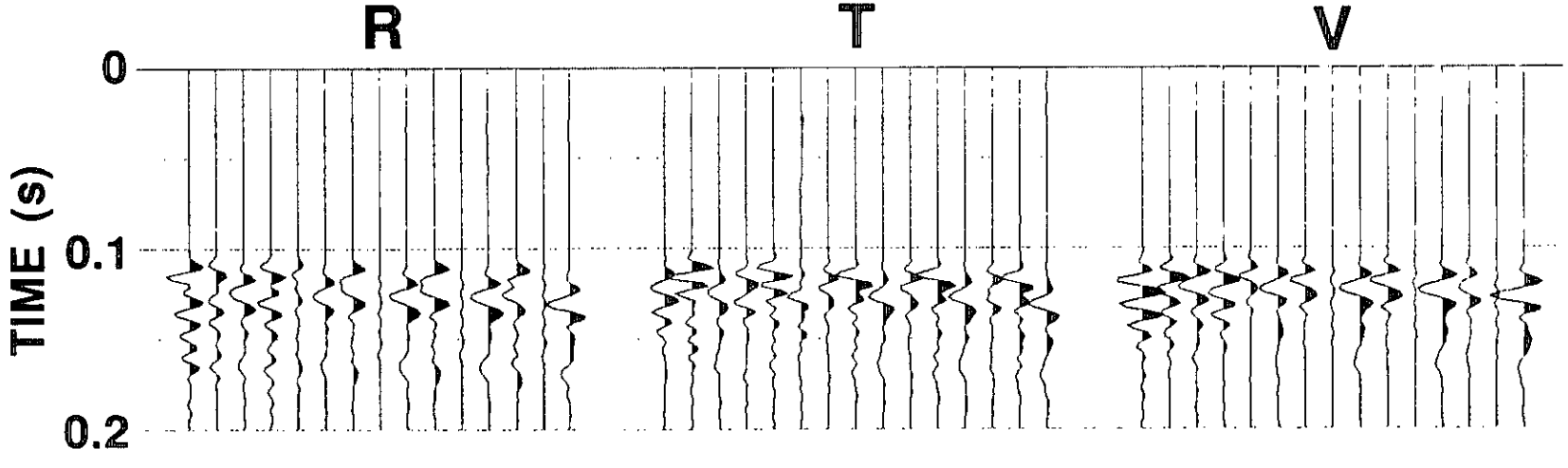

Figure 6. Processed field data from the shotpoint at 90 degrees. Trace order as for Figure 4.

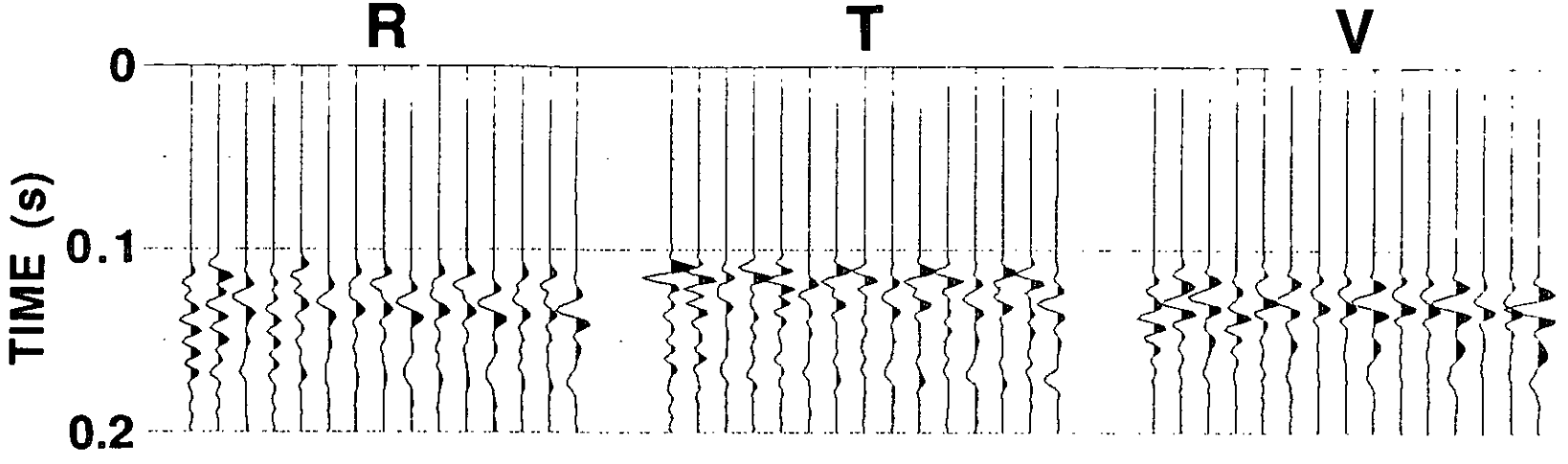

Figure 7. Processed field data from the shotpoint at 135 degrees. Trace order as for Figure 4.

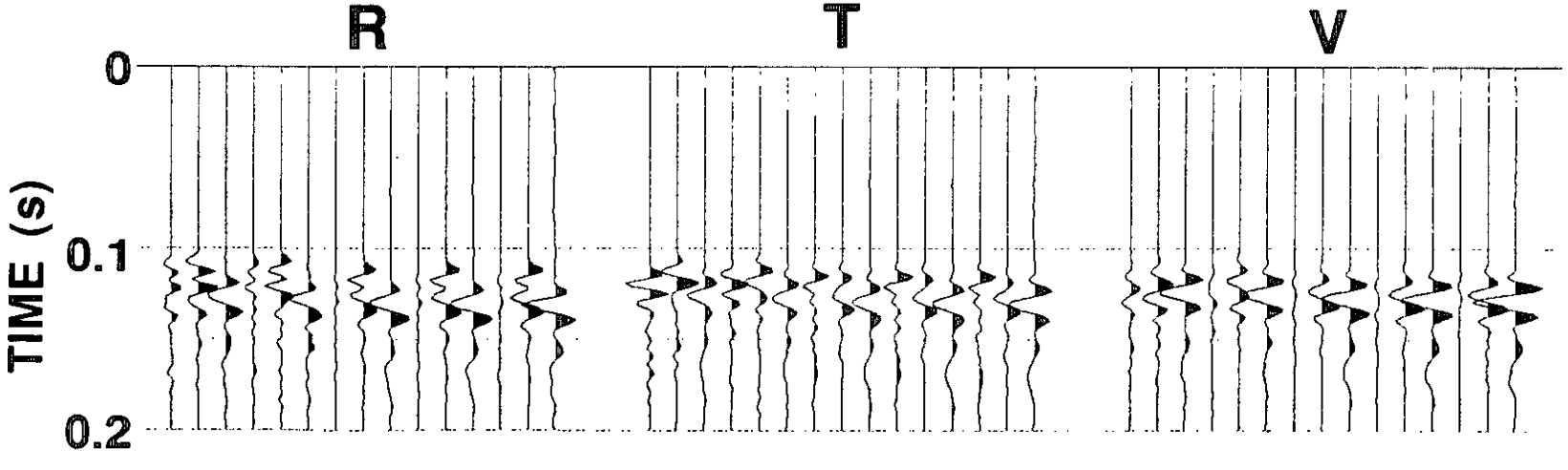

Figure 8. Processed field data from the shotpoint at 180 degrees. Trace order as for Figure 4.

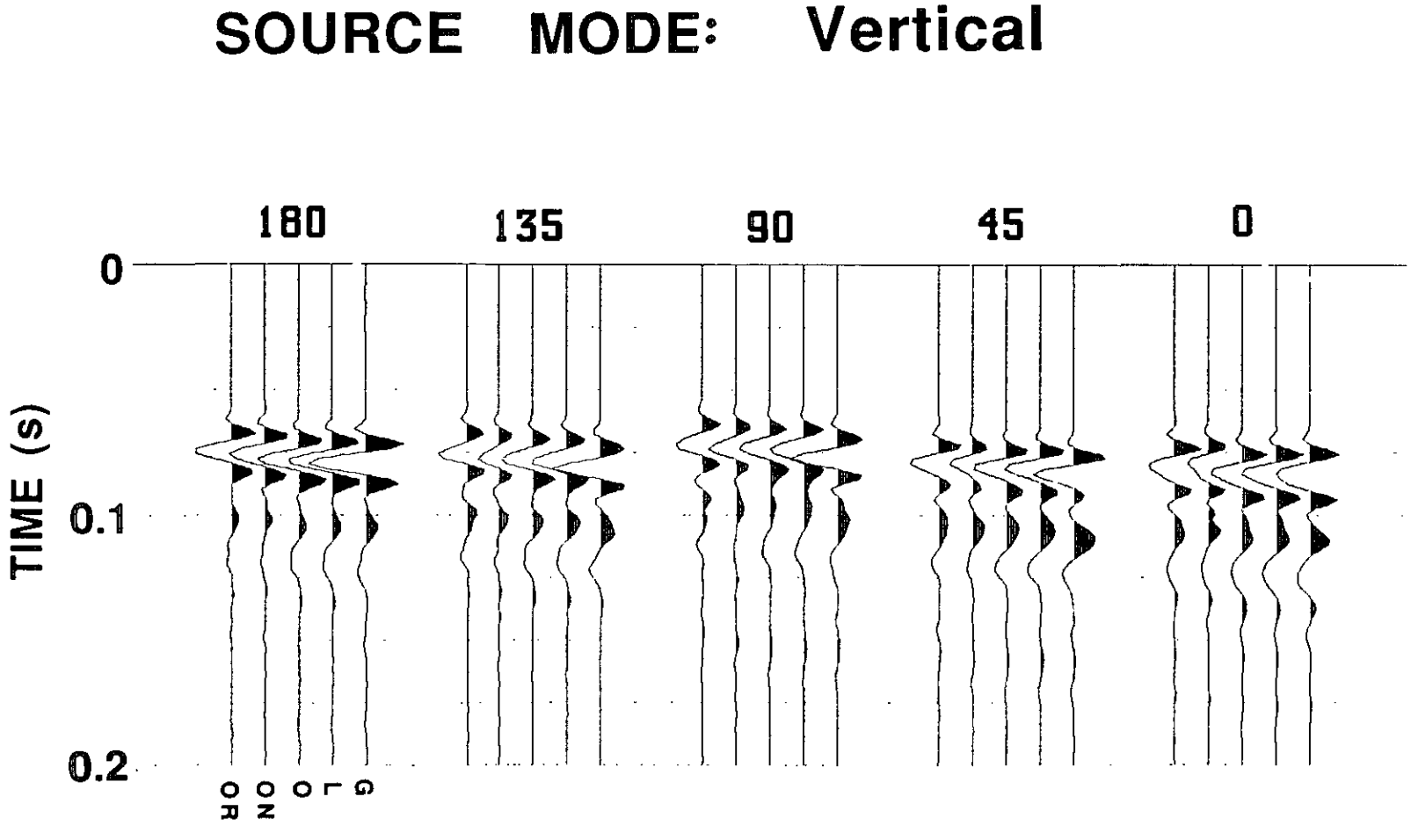

Figure 9. Vertical common component gathers for all shotpoints. The trace order for each panel (right to left) is: Geosource (G), Litton (L), Oyo (O), Omni-n (ON) and Omni-r (OR).

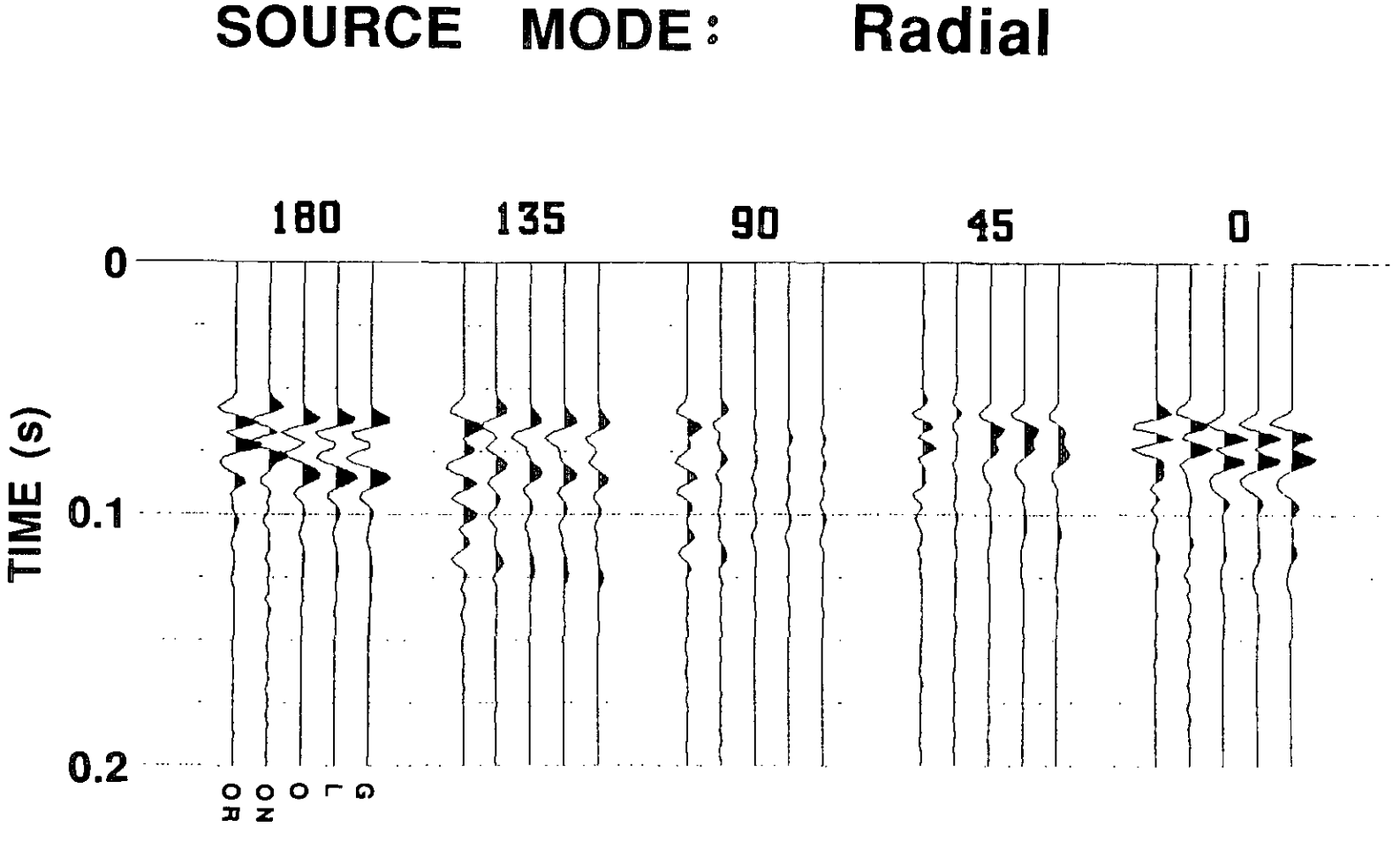

Figure 10. H1 common component gathers for all shotpoints. Trace order as for Figure 9.

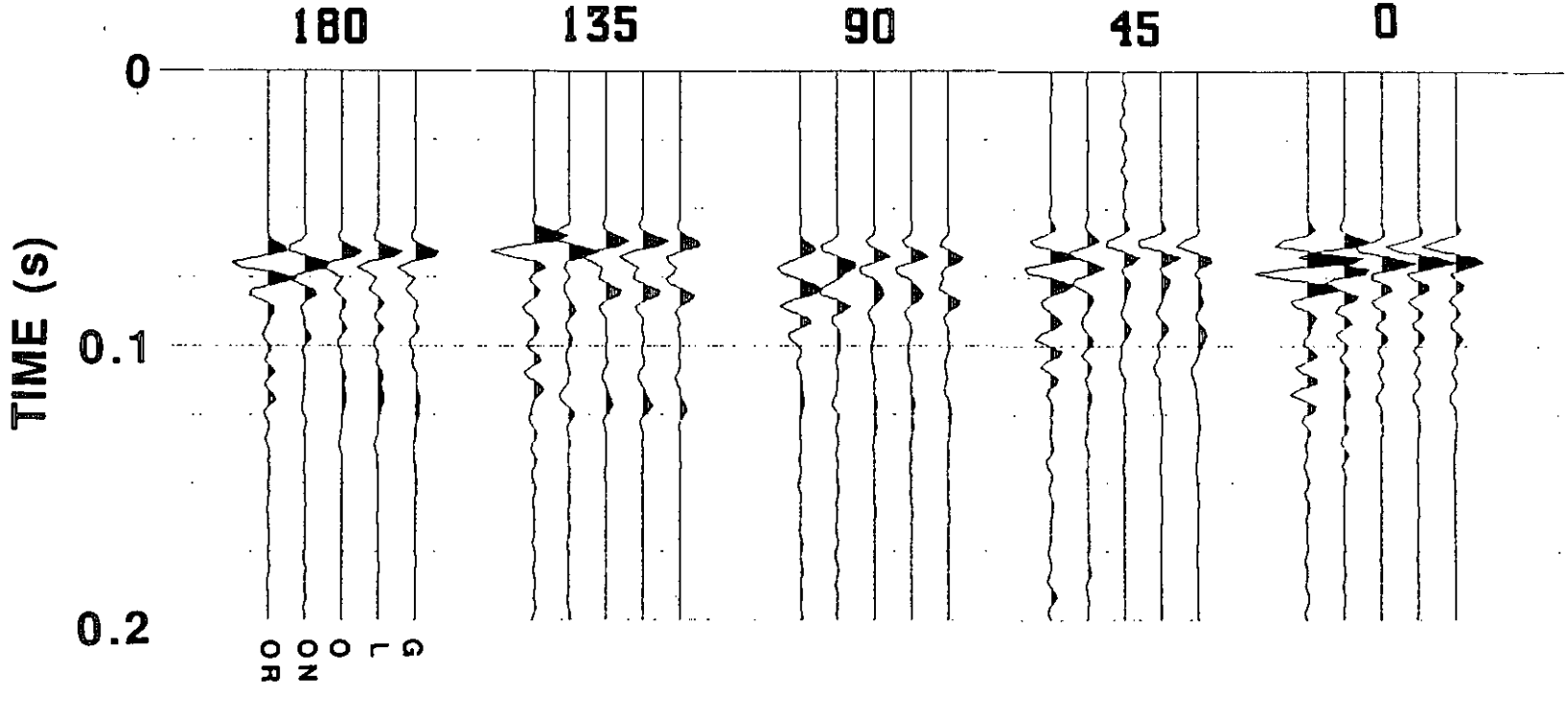

Figure 11. H2 common component gathers for all shotpoints. Trace order as for Figure 9.

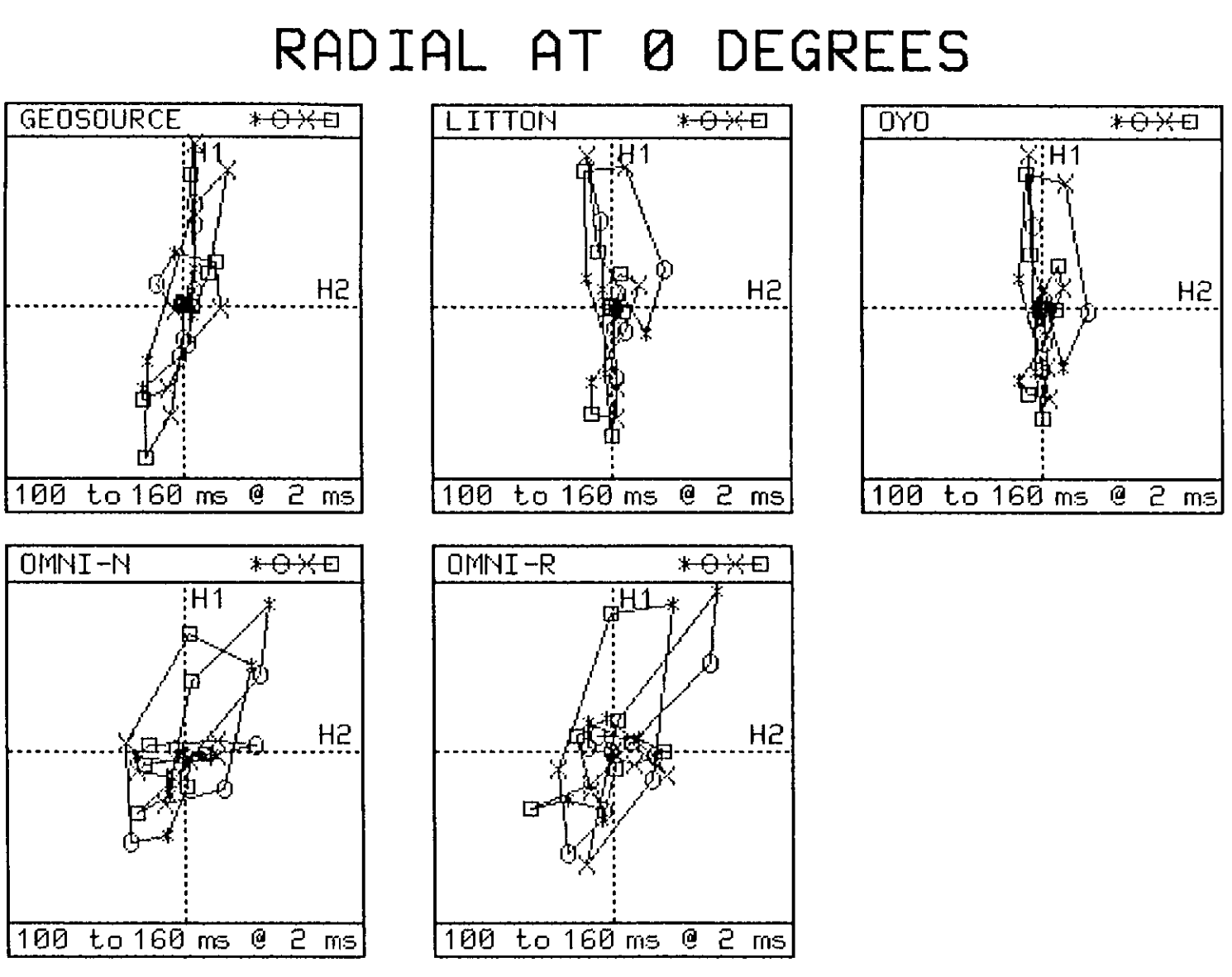

Figure 12. **H1 vs. H2 hodograms for the radial source mode at 0 degrees.**

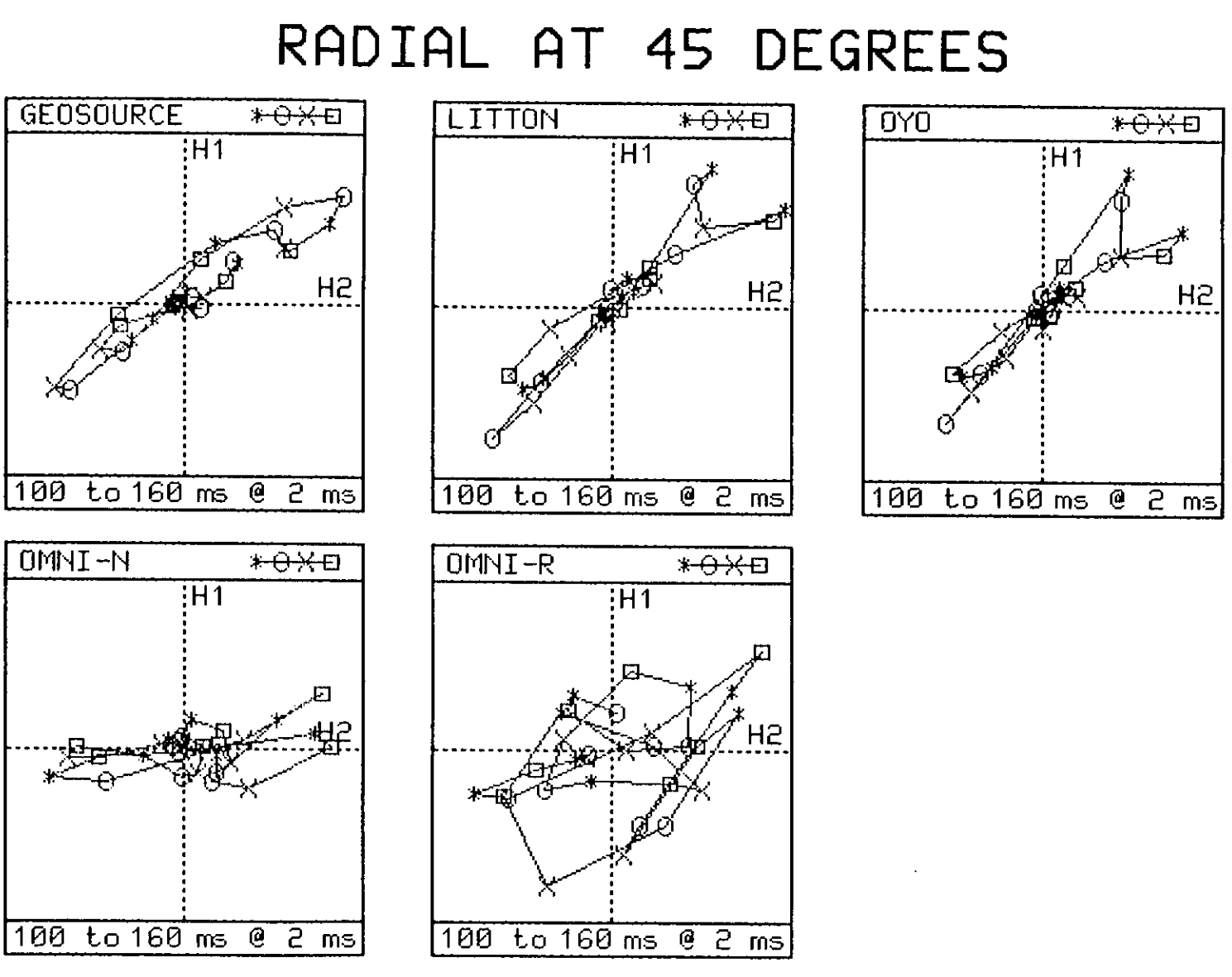

Figure 13. **H1 vs. H2 hodograms for the radial source mode at 45 degrees.**

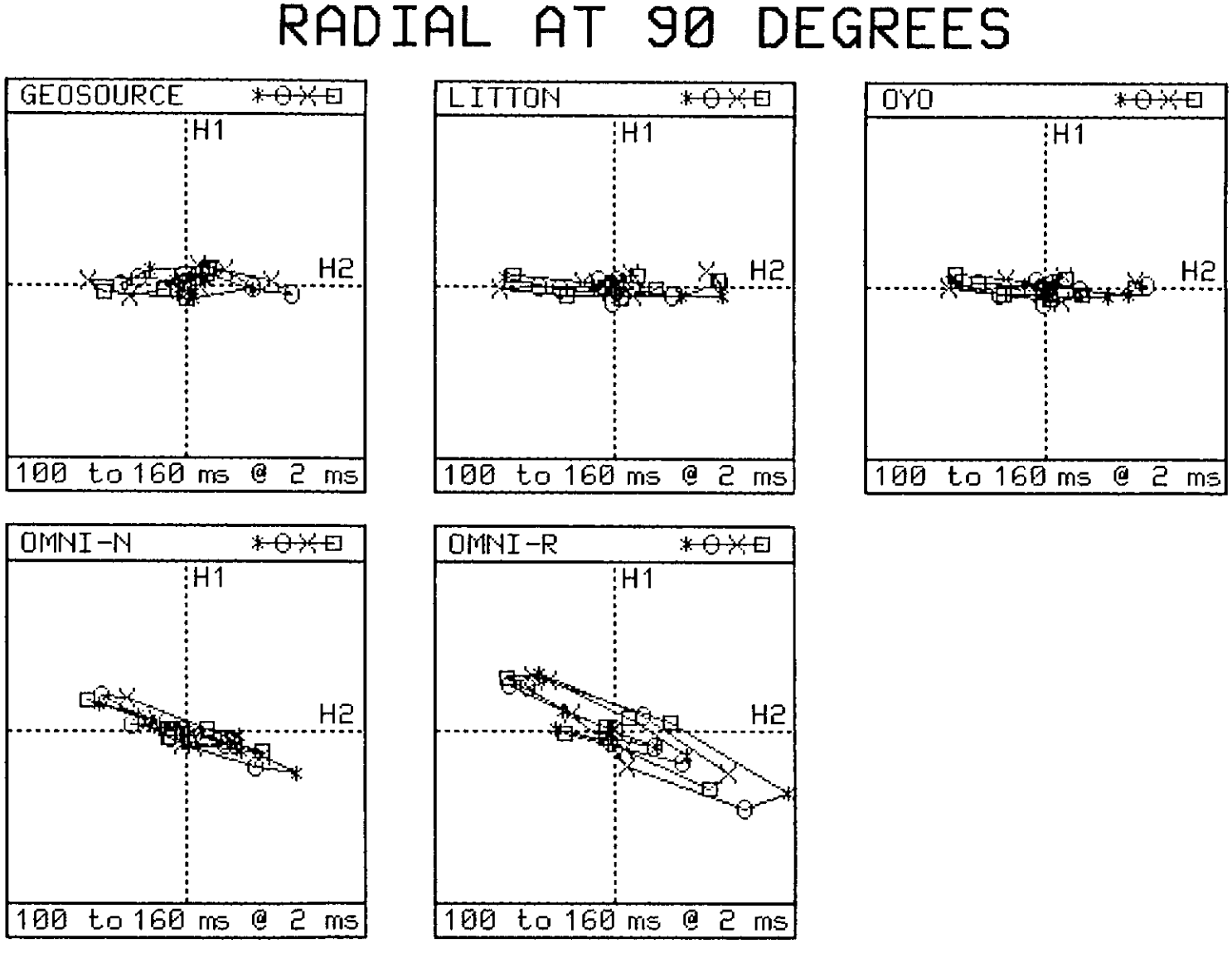

Figure 14. **H1 vs. H2 hodograms for the radial source mode at 90 degrees.**

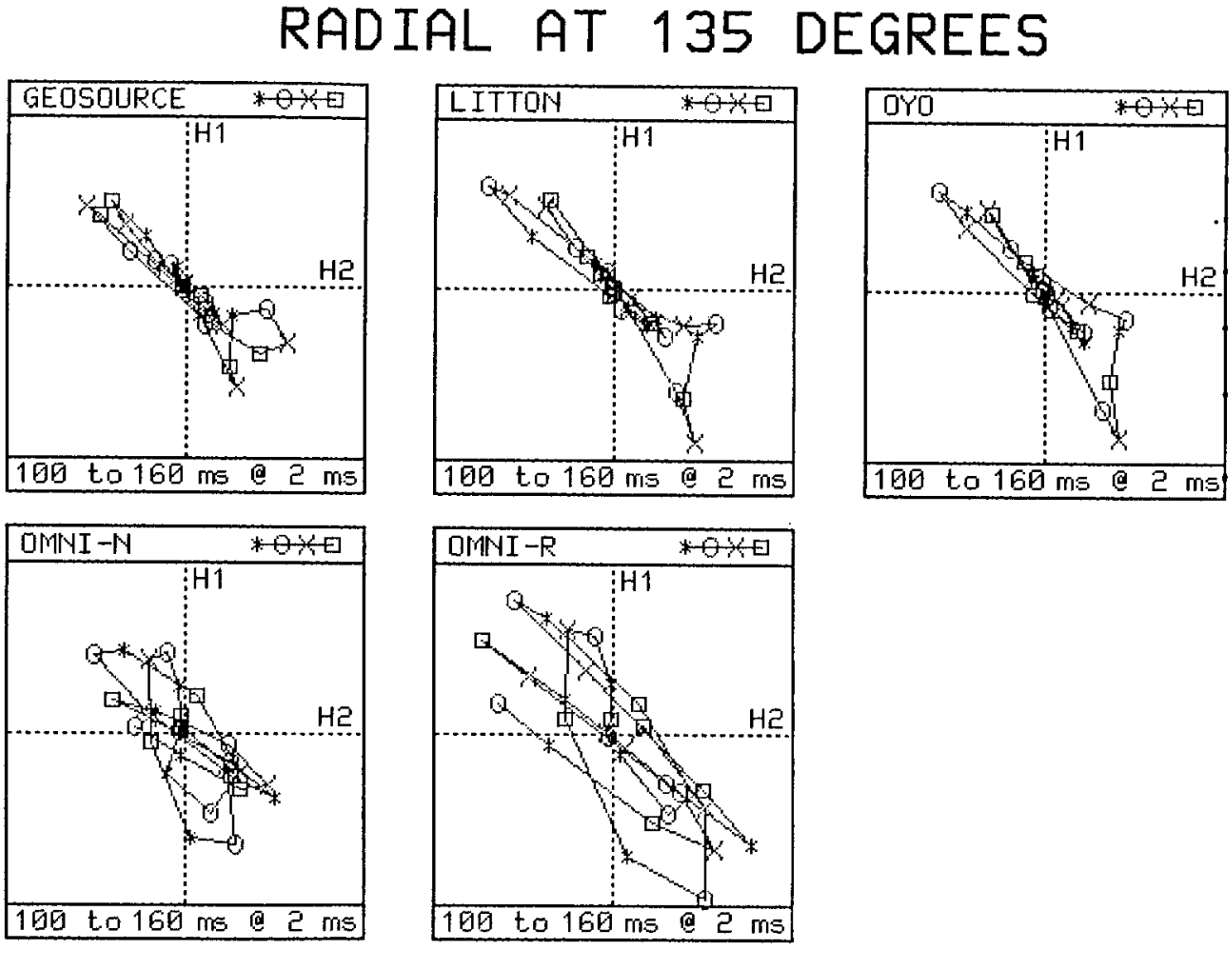

Figure 15. **H1 vs. H2 hodograms for the radial source mode at 135 degrees.**

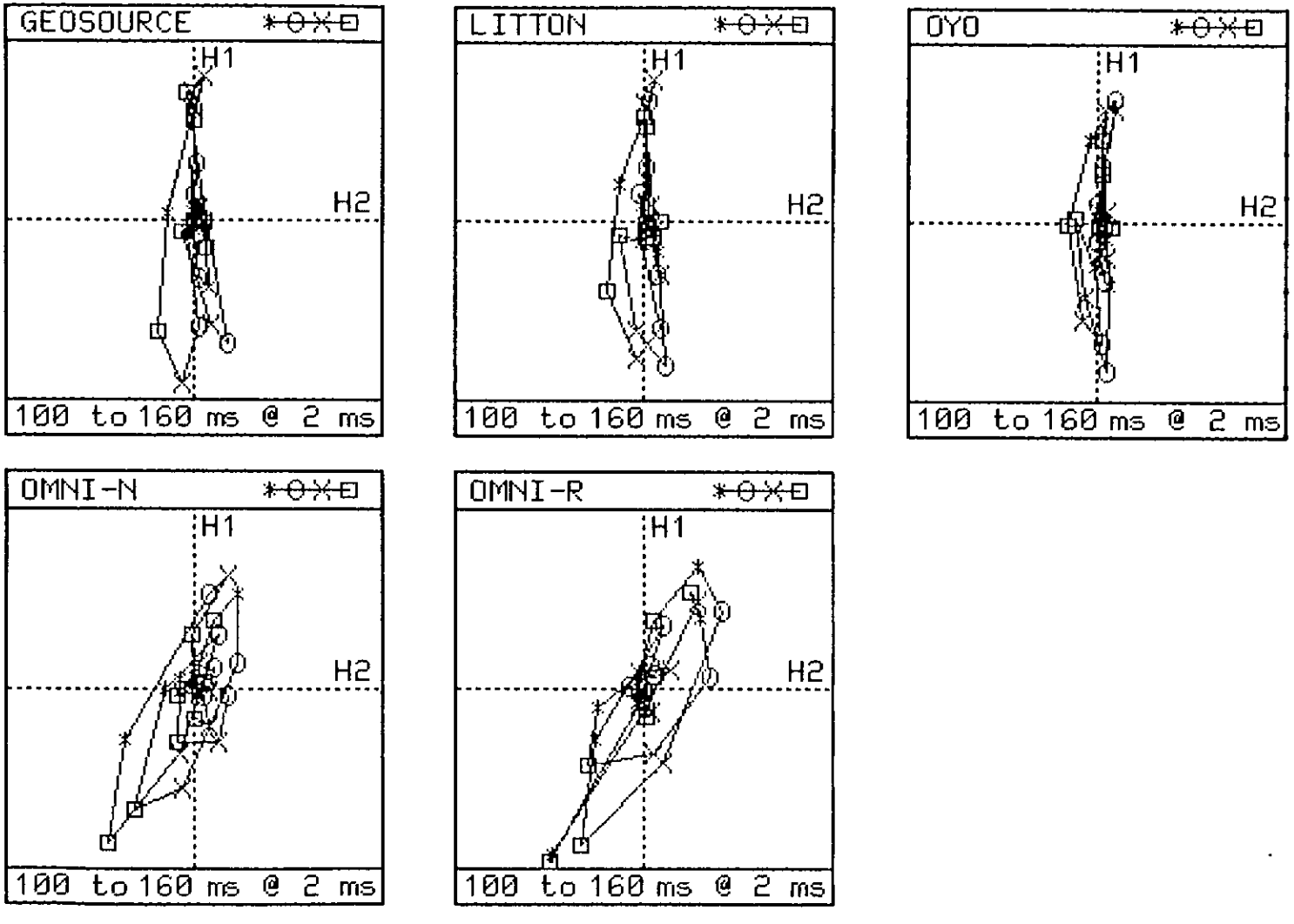

Figure 16. **H1 vs. H2 hodograms for the radial source mode at 180 degrees.**

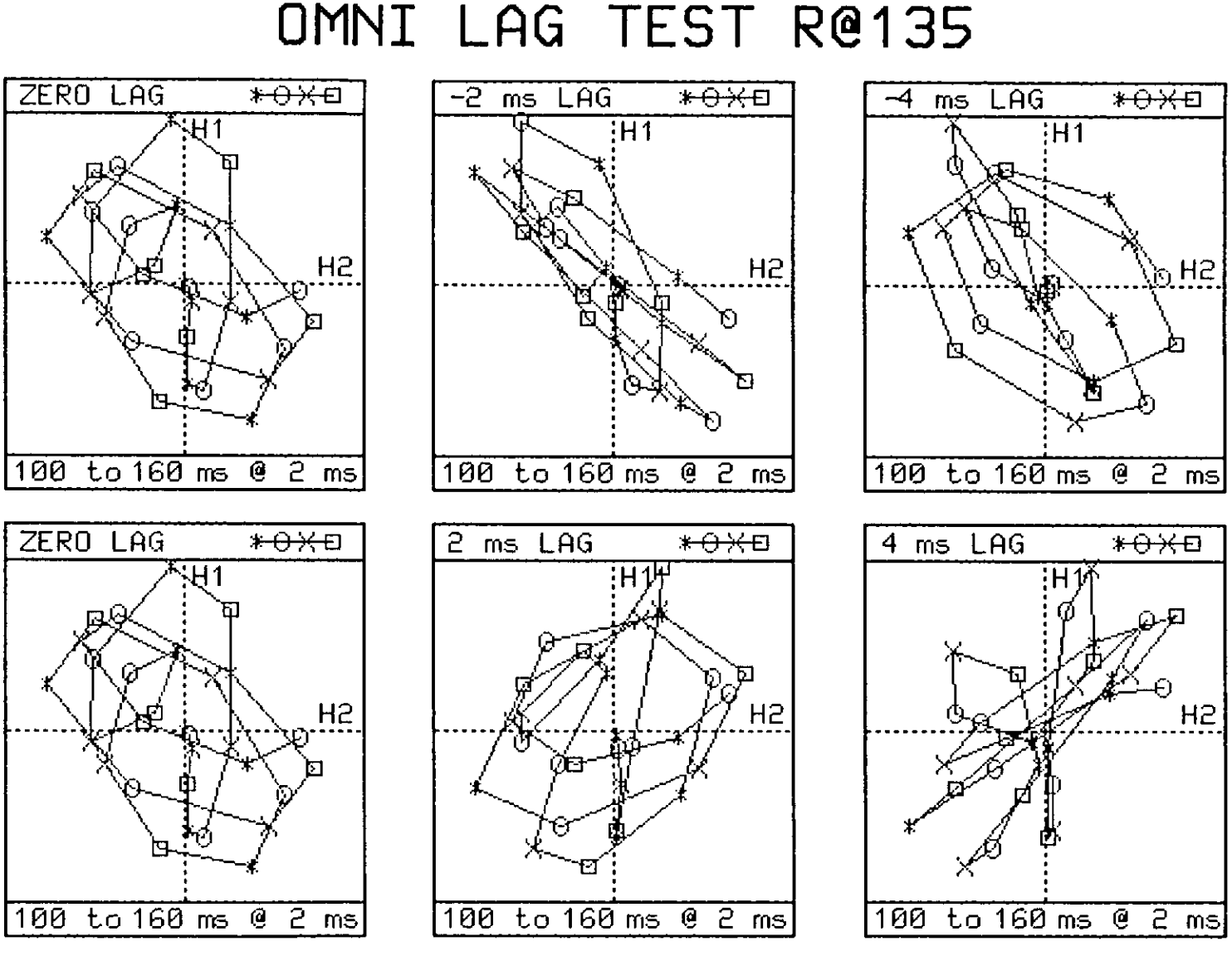

Figure 17. **Lag tests for Omni-r for the radial source mode at 135 degrees. Note the maximum particle motion linearity for a lag of -2ms.**

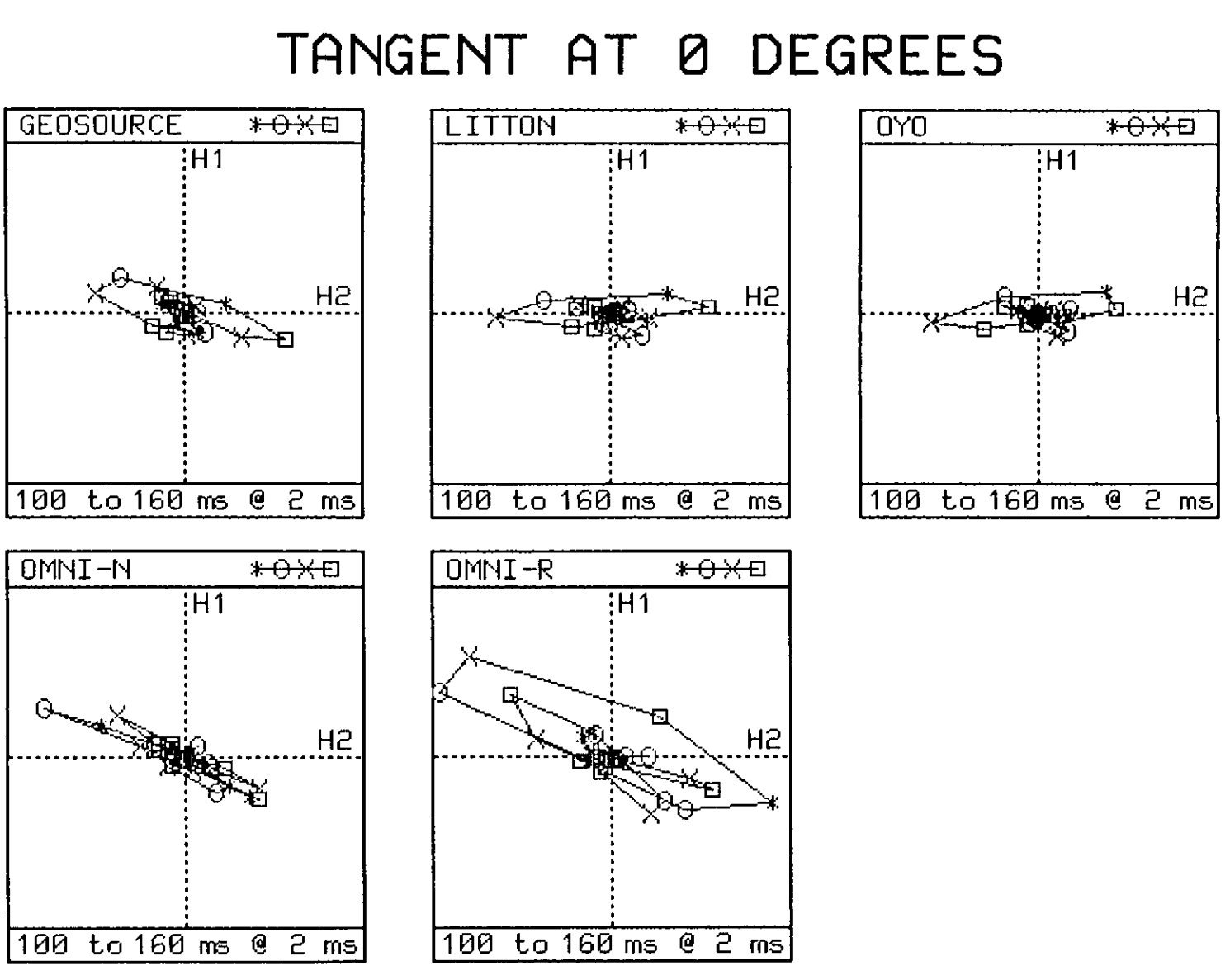

Figure 18. **H1 vs. H2 hodograms for the tangential source mode at 0 degrees.**

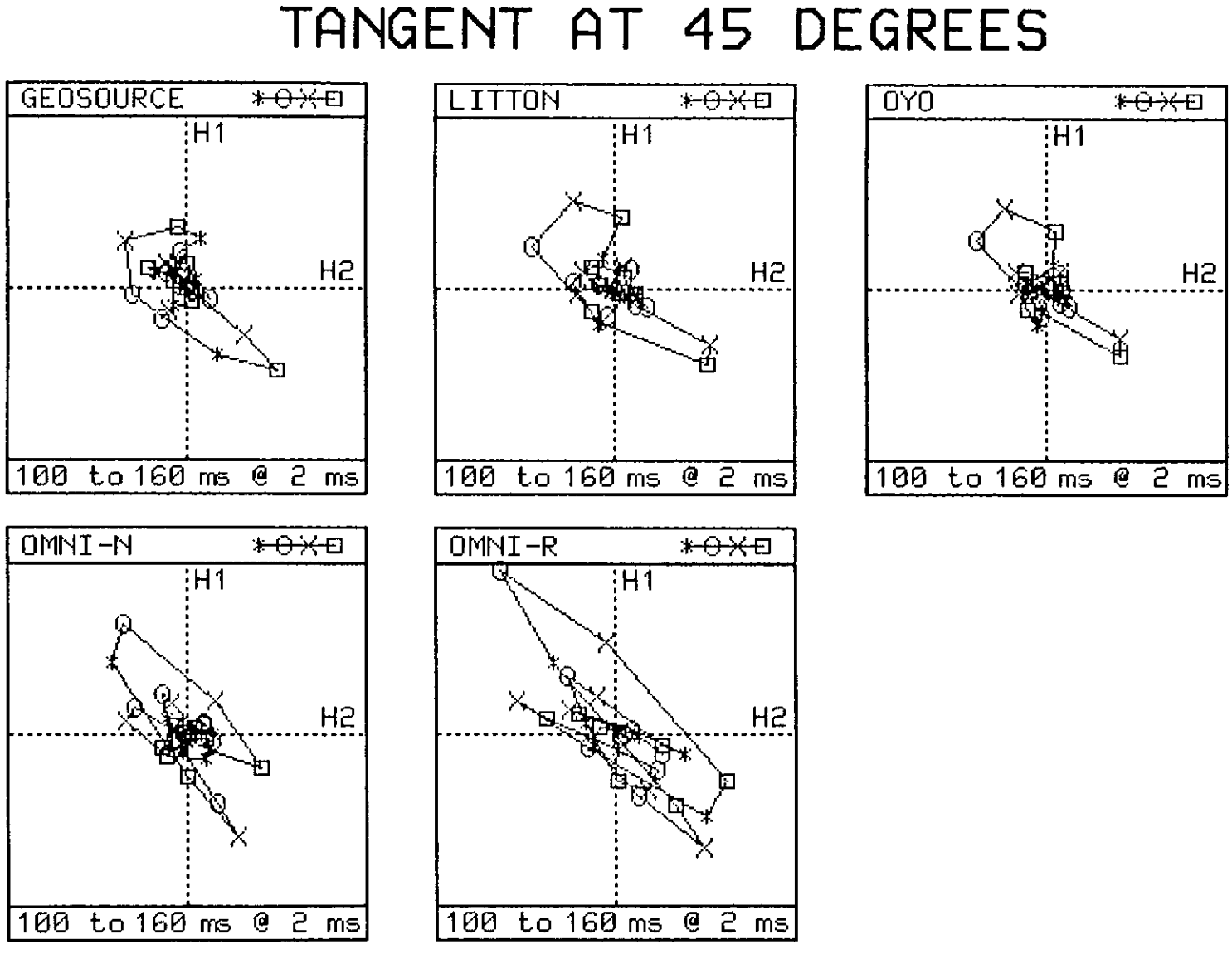

Figure 19. **H1 vs. H2 hodograms for the tangential source mode at 45 degrees.**

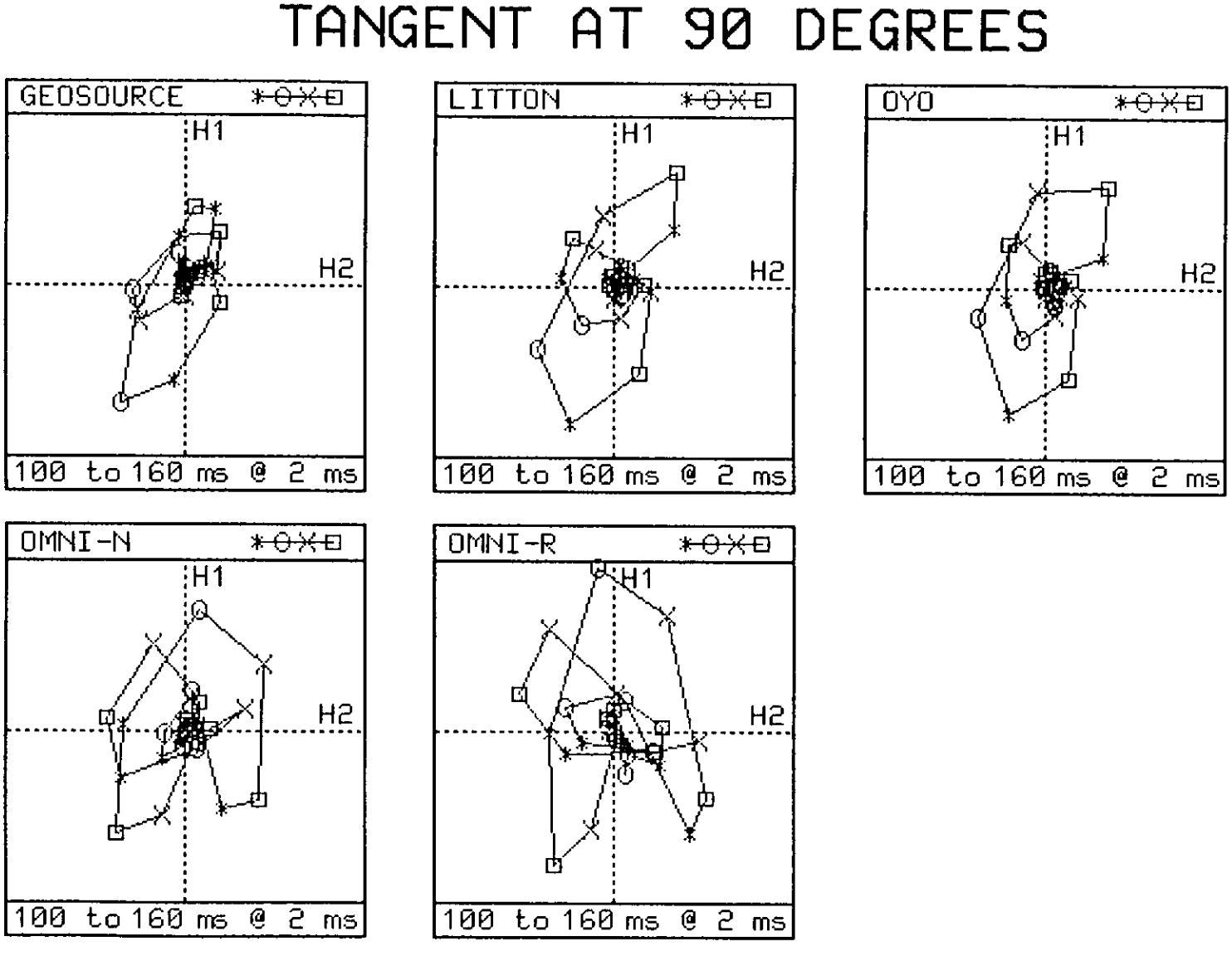

Figure 20. **H1 vs. H2 hodograms for the tangential source mode at 90 degrees.**

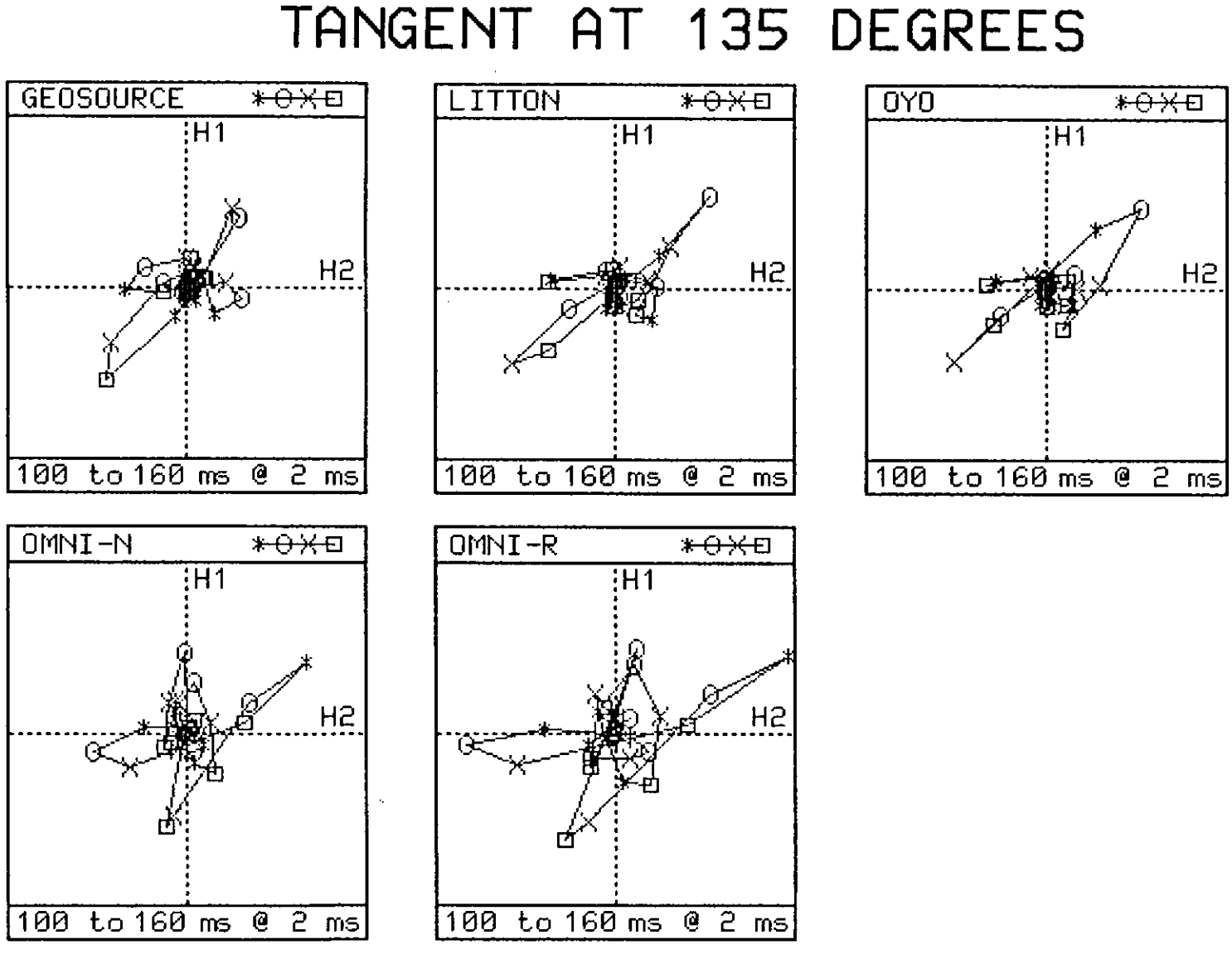

Figure 21. **H1 vs. H2 hodograms for the tangential source mode at 135 degrees.**

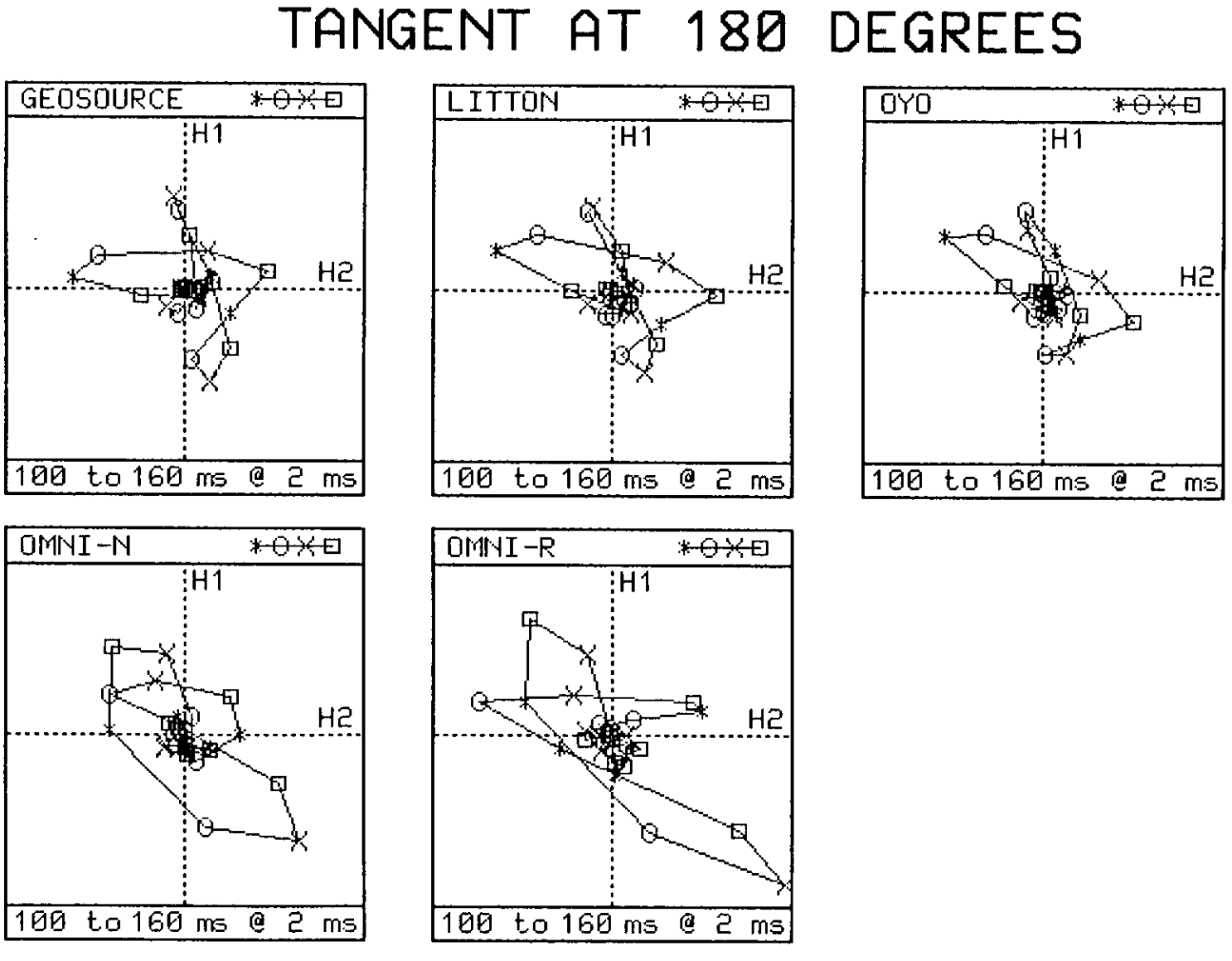

Figure 22. **H1 vs. H2 hodograms for the tangential source mode at 180 degrees.**

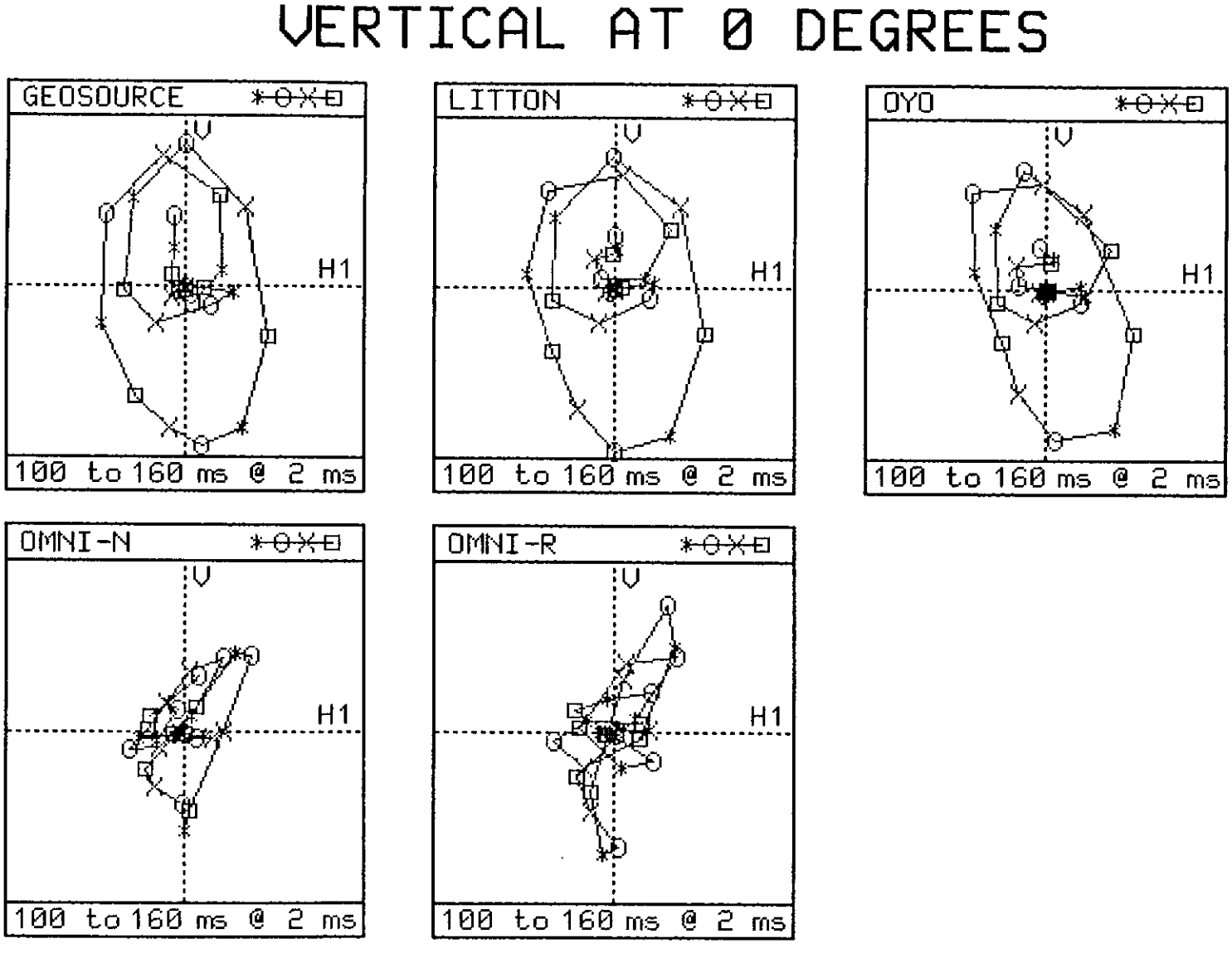

Figure 23. **V vs. H1 hodograms for the vertical source mode at 0 degrees.**

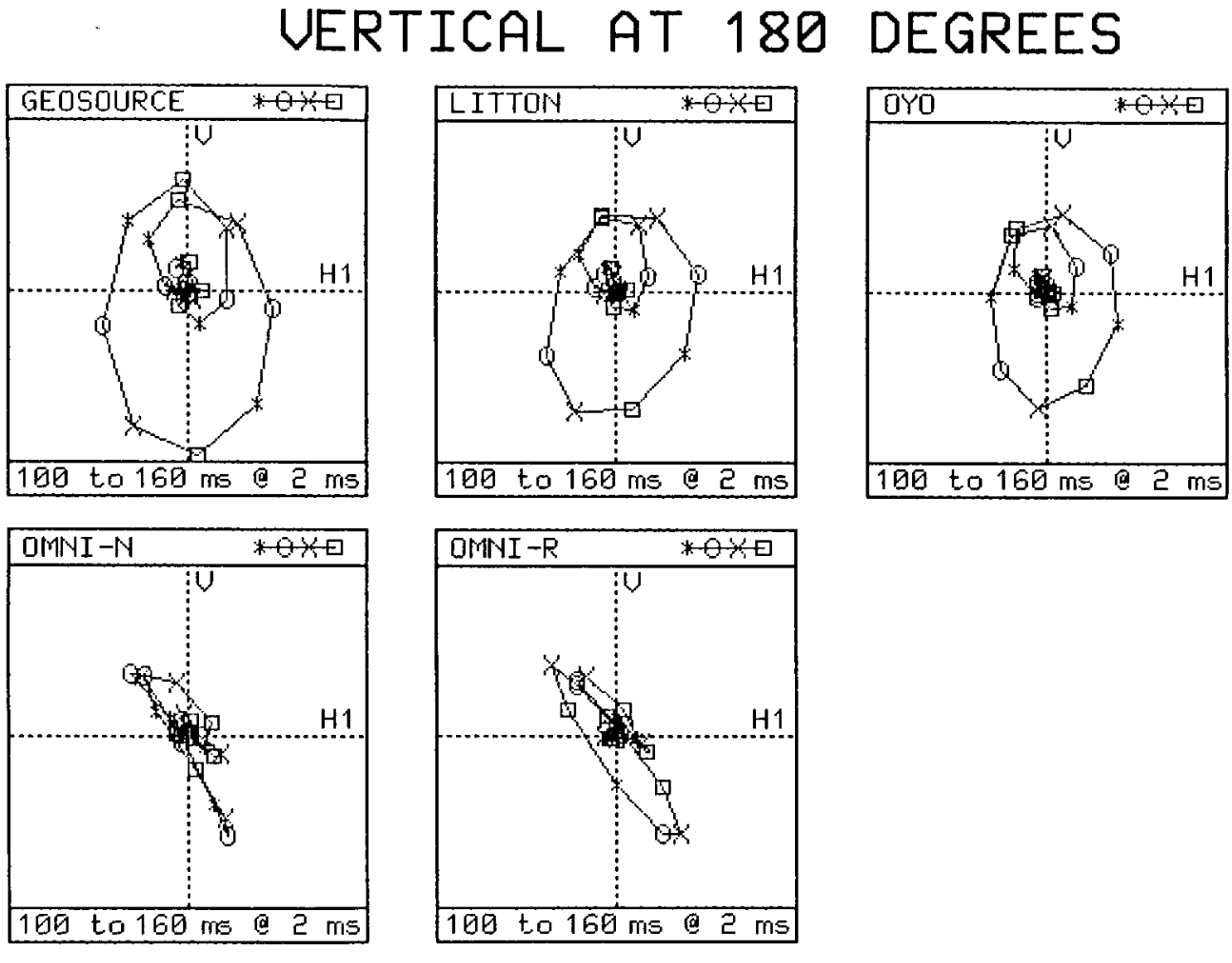

Figure 24. **V vs. H1 hodograms for the vertical source mode at 180 degrees.**

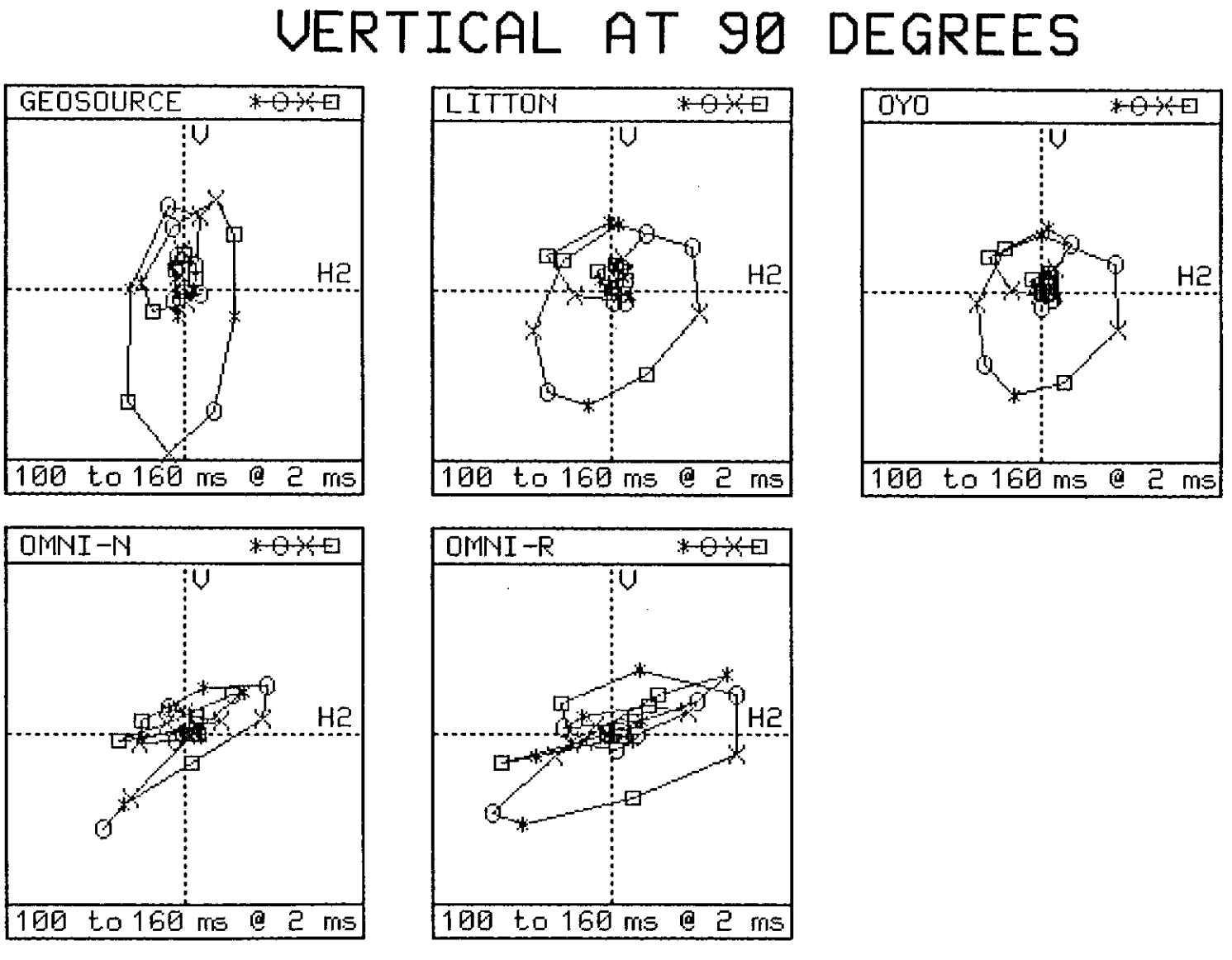

Figure 25. **V vs. H2 hodograms for the vertical source mode at 90 degrees.**